Atmospheric
Chemistry
and Physics

Contrasting impacts of humidity on the ozonolysis of monoterpenes: insights into the multi-generation chemical mechanism

Shan Zhang, Lin Du, Zhaomin Yang, Narcisse Tsona Tchinda, Jianlong Li, and Kun Li

Environment Research Institute, Shandong University, Qingdao 266237, China

Correspondence: Lin Du (lindu@sdu.edu.cn) and Kun Li (kun.li@sdu.edu.cn)

Abstract. Secondary organic aerosol (SOA) formed from the ozonolysis of biogenic monoterpenes is a major source of atmospheric organic aerosol. It has been previously found that relative humidity (RH) can influence the SOA formation from some monoterpenes, yet most studies only observed the increase or decrease in SOA yield without further explanations of molecular-level mechanisms. In this study, we chose two structurally different monoterpenes (limonene with an endocyclic double bond and an exocyclic double bond, Δ^3-carene with only an endocyclic double bond) to investigate the effect of RH in a set of oxidation flow reactor experiments. We find contrasting impacts of RH on the SOA formation: limonene SOA yield increases by $\sim 100\%$ as RH increases, while there is a slight decrease in Δ^3-carene SOA yield. Although the complex processes in the particle phase may play a role, we primarily attribute the results to the water-influenced reactions after ozone attack on the exocyclic double bond of limonene, which leads to the increment of lower volatile organic compounds under high-RH conditions. However, as Δ^3-carene only has an endocyclic double bond, it cannot undergo such reactions. This hypothesis is further supported by the SOA yield enhancement of β-caryophyllene, a sesquiterpene that also has an exocyclic double bond. These results greatly improve our understanding of how water vapor influences the ozonolysis of biogenic organic compounds and subsequent SOA formation processes.

1 Introduction

Secondary organic aerosol (SOA), as an important type of ambient fine particulate matter (PM$_{2.5}$: aerosols with aerodynamic diameter $\leq 2.5\,\mu m$) (Guo et al., 2014; Huang et al., 2014), has caused a series of negative impacts on human health (Pye et al., 2021), air quality (Zhang et al., 2016) and global climate (Levy II et al., 2013). SOA produced from the oxidation of biogenic volatile organic compounds (BVOCs) is a major component of SOA in heavy forest regions during summer (Sindelarova et al., 2014; Ahmadov et al., 2012) and contributes a large fraction ($\sim 40\%$–80%) of the global OA budget (Cholakian et al., 2019).

Monoterpenes, mostly emitted from coniferous trees, account for $\sim 11\%$ of total BVOCs (Sindelarova et al., 2014; Kanakidou et al., 2005). Limonene is one of the most abundant monoterpenes, with an annual emission budget of 11.4 Tg yr^{-1} (Guenther et al., 2012). Apart from the biogenic source, limonene can also be released from indoor emission, mainly from essential oils (Ravichandran et al., 2018; de Matos et al., 2019; Mot et al., 2022). Limonene has an endocyclic double bond and an exocyclic double bond and is thus more reactive than other monoterpenes towards oxidants such as ozone (O$_3$), the hydroxyl radical (OH), and the nitrate radical (NO$_3$) (Chen and Hopke, 2010; Atkinson and Arey, 2003). Δ^3-carene is another kind of monoterpene that dominates the monoterpene emission from Scots pine (Bäck et al., 2012). Different from limonene, Δ^3-carene contains only one endocyclic double bond, which is similar to most other monoterpenes.

Ozonolysis is an important reaction pathway for limonene and Δ^3-carene. Although reactions with OH and NO$_3$ are faster than that with O$_3$ for both of the monoterpenes (Atkinson, 1991; Khamaganov and Hites, 2001; Chen et al., 2015;

Shaw et al., 2018), the atmospheric concentration of the latter monoterpene is much higher than that of the former (Sbai and Farida, 2019). The contributions of O_3 reactions with limonene and Δ^3-carene to tropospheric degradation are 47 % and 24 %, respectively, in the daytime (Ziemann and Atkinson, 2012). In pristine areas where NO_3 concentration is very low, ozonolysis is also the dominant fate for limonene and Δ^3-carene in the nighttime. In addition, it has been previously found that the ozonolysis of monoterpenes can produce more extremely low-volatility products than OH-initiated oxidation, which contributes a large fraction of the SOA production (Jokinen et al., 2015). For either limonene or Δ^3-carene, the first step of ozonolysis is attacking the endocyclic double bond to form two types of stabilized Criegee intermediates (sCIs) with low energy (Fig. S1 in the Supplement) (Drozd and Donahue, 2011; Chen et al., 2019). The sCI will then trigger a series of chemical reactions, like isomerization, decomposition, and addition reactions. Correspondingly, the major components of Δ^3-carene SOA are caric acid, OH-caronic acid, and caronic acid (Ma et al., 2009; Thomsen et al., 2021), while the major components of limonene SOA are limonaldehyde, keto-limononaldehyde, limononic acid, and keto-limononic acid (Pathak et al., 2012; Wang and Wang, 2021).

Water is ubiquitous in the atmosphere and can affect the formation mechanism of SOA and its relevant physical and chemical properties (Sun et al., 2013). A number of field measurements have shown that the average molecular weight of the water/organic phase and activity coefficient of condensed organics would be changed due to the change in relative humidity (RH) (Seinfeld et al., 2001; Li et al., 2020). In addition, several laboratory studies have demonstrated that RH can influence the ozonolysis of monoterpenes in different ways. Most of those studies have reported either an inhibitory effect or a negligible effect of high RH on the particle formation (Bonn and Moortgat, 2002; Fick et al., 2002; Zhao et al., 2021; Ye et al., 2018). Nevertheless, a few other studies found that high RH can promote SOA formation from the ozonolysis of limonene (Yu et al., 2011; Gong et al., 2018; Xu et al., 2021), but the reason for this promotion effect remains unclear.

To fully examine the effects of water on SOA formation from the ozonolysis of monoterpenes, especially the related chemical processes, we used an oxidation flow reactor (OFR) to investigate the ozonolysis of limonene and Δ^3-carene under different RH conditions in this study. An ultra-high-performance liquid chromatography with quadrupole time-of-flight mass spectrometry (UPLC-Q-TOF-MS) instrument was deployed to analyze the molecular chemical composition of the SOA, which provided insights into the physical and chemical processes influenced by the water content. With these state-of-the-art techniques, we proposed mechanisms that may explain the inhibitory or enhancing RH effects on SOA formation for different monoterpenes.

2 Experimental methods

2.1 Oxidation flow reactor experiments

A series of dark ozonolysis experiments of limonene and Δ^3-carene were conducted in a custom-made oxidation flow reactor (OFR). The OFR is a 602 mm long stainless cylinder with a volume of 2.5 L (Fig. S2) (Liu et al., 2014, 2019). A zero-air generator (XHZ2000B, Xianhe, China) was used to generate dry clean air as the carrier gas for the OFR. As shown in Fig. S2, there are four gas paths upstream of the OFR: the first path is the precursor gas channel through which monoterpenes are injected via a syringe pump (IS-PLab 01, DuKe, China), the second path is for the flow of 300 sccm dry zero air passing through a mercury lamp ($\lambda = 185$ nm) to generate O_3, the third path is connected to a water bubbler to generate wet air, and the fourth path is the extra-dry zero air entering the OFR. The RH in the OFR was controlled by adjusting the ratio of the wet and dry zero air flows. A water recycle system was equipped to keep the temperature (T) at around 298 K. The total flow was 0.9 L min^{-1}, resulting in an average residence time of 167 s. The RH and T in the OFR were monitored by a T/RH Sensor (HM40, VAISALA, Finland). The concentration of ozone and the consumption of the precursor gas were measured with an ozone monitor (Model 106L, 2B Technologies, USA) and a gas chromatograph with a flame ionization detector (GC-FID 7890B, Agilent Technologies, USA), respectively. The GC was equipped with a DB-624 column (30 m × 0.32 mm, 1.8 µm film thickness), whose temperature was set to ramp up from 100 to 180 °C at a rate of 20 °C min^{-1}, and then held at 180 °C for 2 min. Before each experiment, O_3 was introduced into the OFR to clean it until the background aerosol mass concentration reached < 1 µg m^{-3}.

The experimental conditions are shown in Table 1. In these OFR experiments, the precursor (limonene or Δ^3-carene) concentration was set to ~ 320–340 ppb. A high O_3 concentration of ~ 6 ppm was used to realize an equivalent aging time of 0.41 d in the real atmosphere, assuming an average ambient O_3 concentration of 28 ppb (Sbai and Farida, 2019) (see Sect. S1 in the Supplement for the calculation). Under such conditions, most of the precursors were consumed, since the residence time was almost 5 and 3 times the half-life for limonene and Δ^3-carene, respectively. Correspondingly, the O_3 consumption for limonene and Δ^3-carene was ~ 250 and ~ 100 ppb, respectively. A series of RH conditions ranging from dry (1 %–2 %) to 60 % with a step of ~ 10 % were used to investigate the effects of water content on SOA production and composition (see Table 1). All materials used in the experiments have been described in Sect. S2.

Table 1. Experimental conditions and results.

Exp.	Precursor concentration (ppb)	$[O]_3$ (ppm)	T (K)	RH (%)	$N^a_{(13.8–723.4\,nm)}$ (cm^{-3})	$M^b_{(13.8–723.4\,nm)}$ (µg m^{-3})	$D^c_{(mean)}$ (nm)	SOA yield (%)
Limonene								
1	321 ± 39	5.7	298	1–2	6.9×10^5	980.9	138.2	62.9
2	321 ± 39	6.0	298	10 ± 2	1.3×10^6	1377.5	126.8	88.4
3	321 ± 39	5.9	298	20 ± 2	9.0×10^5	1573.3	150.9	90.2
4	321 ± 39	5.9	298	30 ± 2	1.4×10^6	1573.3	128.9	100.9
5	321 ± 39	6.0	298	40 ± 2	1.7×10^6	2051.4	130. 7	131.6
6	321 ± 39	5.5	298	50 ± 2	1.5×10^6	1962.7	137.8	125.9
7	321 ± 39	5.5	298	60 ± 2	1.5×10^6	2211.1	139.0	141.8
Δ^3-carene								
8	341 ± 28	6.1	298	1–2	9.5×10^4	346.0	195.8	19.4
9	341 ± 28	6.4	298	10 ± 2	1.4×10^5	300.3	163.4	16.8
10	341 ± 28	6.4	298	20 ± 2	9.4×10^4	244.9	176.9	13.7
11	341 ± 28	6.0	298	30 ± 2	5.9×10^4	241.2	205.1	13.5
12	341 ± 28	6.3	298	40 ± 2	4.6×10^4	205.8	203.2	11.5
13	341 ± 28	6.3	298	50 ± 2	6.8×10^4	196.7	180.7	11.0
14	341 ± 28	6.3	298	60 ± 2	5.6×10^4	198.5	190.2	11.1

[a] $N_{(14.1–735\,nm)}$ means the total particle number concentration from size 13.8 to 723.4 nm. [b] $M_{(13.8–723.4\,nm)}$ means the total particle mass concentration from size 13.8 to 723.4 nm. [c] $D_{(mean)}$ means the particle mean diameter.

2.2 SOA particle analysis

2.2.1 SOA yield

The SOA particle size distribution was measured with a scanning mobility particle sizer (SMPS), which consists of a differential mobility analyzer (DMA) (model 3082, TSI Inc., USA) and a condensation particle counter (CPC) (model 3776, TSI Inc., USA). The samples were measured by SMPS every 5 min with a sampling flow and a sheath flow of 0.3 and 3 L min^{-1}, respectively. The SOA mass concentration was calculated from the volume concentration measured with SMPS and the aerosol density, which was estimated to be 1.25 cm^{-3} for limonene SOA and 1.09 g cm^{-3} for Δ^3-carene SOA (Thomsen et al., 2021; Watne et al., 2017).

The SOA yield (Y) for individual organic gas can be calculated as

$$Y = \frac{\Delta M}{\Delta HC}, \tag{1}$$

where ΔM is the total mass concentration of SOA, and ΔHC is the mass concentration of reacted precursor (Ng et al., 2007; Odum et al., 1996).

2.2.2 Ultra-high-performance liquid chromatography with quadrupole time-of-flight mass spectrometry analysis

An ultra-high-performance liquid chromatography system (UPLC, UltiMate 3000, Thermo Scientific) coupled with a quadrupole time-of-flight mass spectrometry instrument (Q-TOF-MS, Bruker Impact HD) was used to analyze the molecular-level chemical composition of SOA. First, the SOA particles were collected on the PTFE filters (47 mm diameter, 0.22 µm pore size, Jinteng, China). Next, these filters were dissolved and extracted by 5 mL methanol twice. Extracts were then filtered through PTFE syringe filters (0.22 µm pore size) and were concentrated to near dryness by nitrogen blowing. Finally, the samples were redissolved in a 200 µL solution with 0.1 % (v/v) formic acid in a 50 : 50 methanol / ultrapure water mixture.

The parameters of the LC–MS instrument were set as follows: capillary voltage 4000 V, nebulizer pressure 0.4 bar, dry heater temperature 200 °C, end plate voltage −500 V, and flow of dry gas 4 L min^{-1}. A C$_{18}$ column (100 Å, 3 mm particle size, 2.1 mm × 50 mm; Waters, USA) was used with a column temperature of 35 °C. The mobile phase was 0.1 % formic acid in methanol (A) and 0.1 % formic acid in ultra-high-purity water (B) with a flow of 200 µL min^{-1}. The injection volume was 5 µL. The mass spectrometer was operated in negative ion mode, and the detection molecular weight range was from m/z 50 to 1500. The temperature ramping program was 0–3 min with 0 %–3 % phase B, 3–25 min with 3 %–50 % phase B, 25–43 min with 50 %–90 % phase B, 43–48 min with 90 %–3 % phase B, and 48–60 min with 3 % phase B.
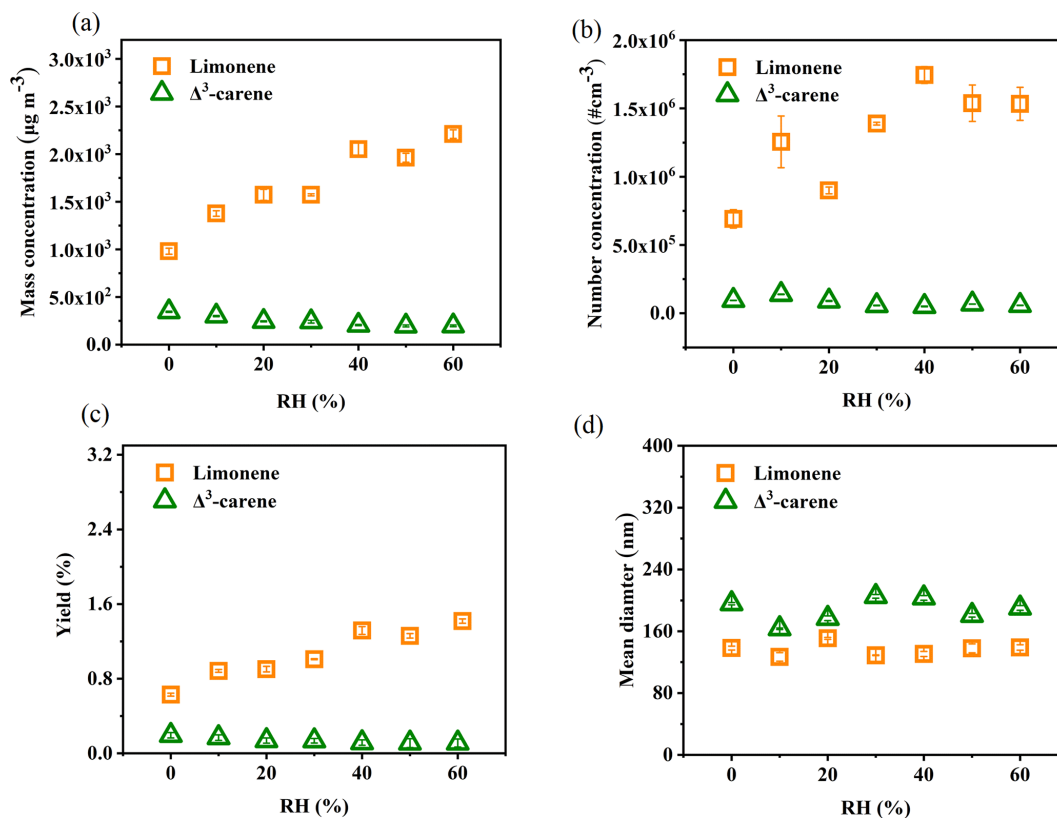
Figure 1. The effect of RH on the SOA formation: **(a)** number concentration, **(b)** mass concentration, **(c)** SOA yield, and **(d)** mean diameter.

3   Results and discussion

3.1   SOA production under different RH conditions

The SOA formation of a representative experiment is shown in Fig. S3. It is found that the formed SOAs are mainly in the size range of 60–200 nm, and the number concentration and mass concentration are relatively stable during the course of the OFR experiment. SOA formation from limonene and Δ^3-carene in terms of particle number concentration, particle mass concentration, and SOA yield as a function of RH is illustrated in Fig. 1a–c. We find that all three of the above-mentioned parameters of limonene SOA increase with the increasing RH. The increment of particle mass concentration and SOA yield from the ozonolysis of limonene is $\sim 100\%$ higher at wet (60 % RH) than at dry conditions. In contrast, SOA formation from Δ^3-carene is suppressed by $\sim 40\%$ under high RH. The distinct effects of RH on SOA formation from the ozonolysis of limonene and Δ^3-carene found in this study agree with most previous studies (Yu et al., 2011; Jonsson et al., 2006; Bonn et al., 2002; Gong and Chen, 2021; X. Li et al., 2019). As shown in Table 2, Yu et al. (2011) reported a positive correlation between SOA production and RH for the ozonolysis of limonene in the chamber experiments without OH scavenger. Their experimental condition is similar to that in our study regarding the absence of OH

scavenger, and, thus, similar results were observed. However, in the presence of OH scavenger, results are quite different. Jonsson et al. (2006) observed a similar enhancement effect of high RH on SOA production with 2-butanol to the OH scavenger, while Bonn et al. (2002) found a negligible or suppressive effect with cyclohexane as the OH scavenger. It should be noted that the OH scavenger not only has the ability to scavenge OH but also produces additional products which may influence the reactions of target precursors. For example, there is no difference between 2-butanol and cyclohexane in the scavenging ability of the OH radical, though 2-butanol will produce more $HO_2\cdot$ than cyclohexane, and, consequently, $R\cdot$ will react with $HO_2\cdot$ to produce more hydroxyl acids and hydroxyl per-acid products, most of which have low volatility, and thus they partition into the particle phase. According to previous studies, the influence of different OH scavengers can vary (Jonsson et al., 2008). This may explain the different findings with and without OH scavenger for limonene SOA. With regard to Δ^3-carene, similar results are found in the absence of OH scavenger, namely, high RH has negligible or slightly suppressive effect on SOA production (Bonn et al., 2002; Fick et al., 2002). The same as limonene, the presence of OH scavenger and its different chemical nature can explain the different results found previously (Jonsson et al., 2006; Bonn et al., 2002).

Table 2. Comparison with previous studies on the effect of RH.

Precursor	Precursor concentration (ppb)	O_3 concentration (ppb)	Reactor	OH scavenger	T (K)	RH (%)	SOA mass concentration (μg m^{-3})	SOA yield (%)	M[a]	N[b]	Reference
limonene	1000	1000	flow reactor	cyclohexane	295 ± 2	0.02 and 32.5	N.M.[c]	N.M.[c]	no effect	−[e]	Bonn et al. (2002)
	320	100 ± 5	chamber	N.M.[c]	296 ± 2	18 ± 2, 50 ± 3 and 82 ± 2	24; 58; 120	7.0 ± 0.7; 17.4 ± 1.3; 53.4 ± 1.9	+[d] (7 times)	+[d] (8 times)	Yu et al. (2011)
	15 and 30	430.9	flow reactor	2-butanol	298 ± 0.4	< 2–85	2.7–10.5 and 62–229	6.8–26.4 and 77.4–285.7	+[d]	+[d]	Jonsson et al. (2006)
	endocyclic (24.6) and exocyclic (15.2)	endocyclic (270) and exocyclic (12 200)	flow reactor	2-butanol	298	10–50	endocyclic ($\sim$11) and exocyclic (22–51)	endocyclic ($\sim$7.4) and exocyclic (23.8–55.3)	exocyclic (+[d]) and endocyclic (−[c])	N.M.[c]	Gong and Chen (2021)
	1085	900 ± 10	flow reactor	none	298	3–62	150; 200; 210	N.M.	+[d]	−[e]	X. Li et al. (2019)
	321 ± 39	5786 ± 203	flow reactor	none	298	0–60	980.9–2211.1	62.9–141.8	+[d] (2 times)	+[d] (3 times)	this study
Δ^3-carene	1000	1000	flow reactor	cyclohexane	295 ± 2	0.02 and 32.5	N.M.[c]	N.M.[c]	no effect	−[e]	Bonn et al. (2002)
	14.2 and 29.4	2300	flow reactor	2-butanol	298 ± 0.4	< 2–85	0.78–3.8 and 15.3–94;	2.1–10.1 and 19.8–116.7	+[d]	+[d]	Jonsson et al. (2006)
	1111	900 ± 10	flow reactor	none	298	3–62	75; 80; 90	N.M.	−[e]	−[e]	X. Li et al. (2019)
	341 ± 28	6257 ± 140	flow reactor	none	298	0–60	346.0–198.5	19.4–11.1	−[e]	no effect	this study

[a] M means the change trend total particle mass concentration. [b] N means total particle number concentration. [c] N.M. means not mentioned. [d] Positive sign (+) means the mass or number concentration increases with RH. [e] Negative sign (−) means the mass or number concentration decreases with RH.
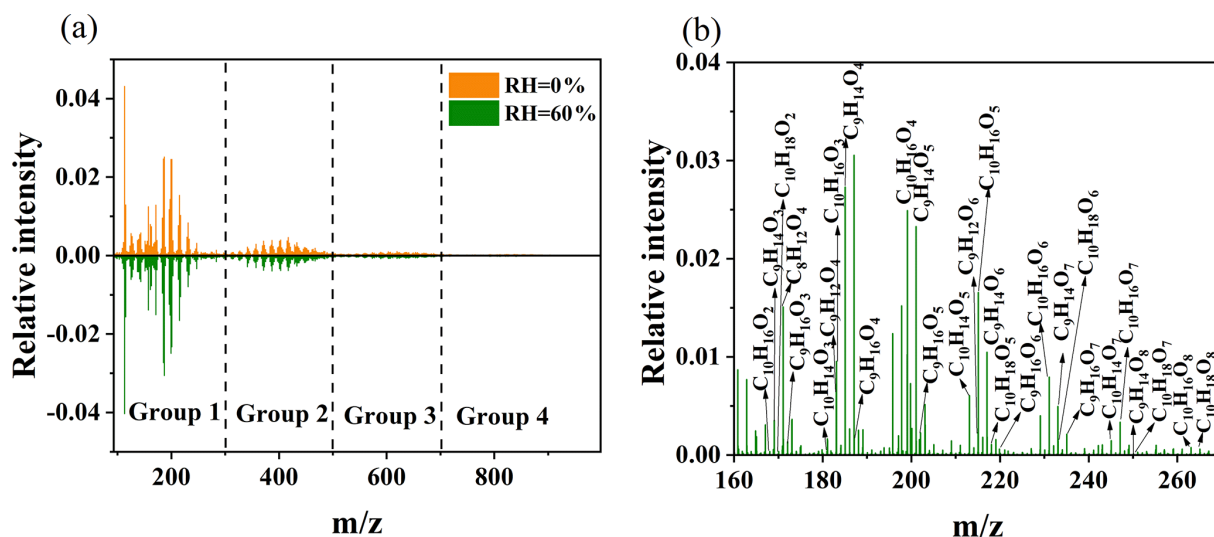
Figure 2. UPLC/(−) ESI-Q-TOF-MS mass spectra of SOA from limonene ozonolysis. **(a)** MS under high- and low-RH conditions and **(b)** the identification of monomers under high-RH conditions.

The enhancement in limonene-SOA production under high RH can be for several reasons from either physical or chemical processes. First, the hygroscopic growth of the particles (i.e., absorption of water content) can lead to higher mass concentration under higher RH, but the enhancement should be at most $\sim 30\%$ as the growth factor (GF; the ratio of wet and dry diameter: $D_{\text{wet}}/D_{\text{dry}}$) of limonene SOA is ≤ 1.1 (Varutbangkul et al., 2006). However, we do not observe an obvious change in the mean diameter when comparing dry and wet conditions (Fig. 1d). In addition, hygroscopic growth should also occur for Δ^3-carene SOA, but no obvious enhancement in particle mass is observed (Fig. 1a). Therefore, it is suggested that physical processes regarding hygroscopic growth play a minor role in the enhancement in limonene SOA under high RH. As a consequence, we believe that chemical processes are likely the reason of the enhancement in limonene SOA under high RH. Water can influence chemical processes in the gas phase or in the particle phase. Particle-phase reactions can promote the growth of small particles and, thus, mainly lead to larger particle sizes. As the observed SOA enhancement is mainly from high number concentration particles rather than the large size particles (Fig. 1b and d), it is likely that the water-participated gas-phase reactions are the most possible reasons for the limonene-SOA enhancement. The reaction mechanism is analyzed below based on the mass spectra information on the SOA.

3.2 Molecular analysis of SOA particles

The UPLC/ESI-Q-TOF-MS was used to examine the SOA molecular composition under high- and low-RH conditions. As shown in Fig. 2a, the mass spectra of limonene SOA are divided into four groups: monomeric group ($< m/z$ 300),

dimeric group (m/z 300–500), trimeric group (m/z 500–700), and tetrameric group (m/z 700–1000), corresponding to products containing one, two, three, and four oxygenated limonene units, respectively (Bateman et al., 2009). Most of the SOA molecules are monomers ($> 60\%$) (Fig. 2b) and dimers ($\sim 25\%$), while trimers and tetramers contribute very small fractions ($< 10\%$ and $\sim 3\%$) (Table S1 in the Supplement). Correspondingly, the distribution of Δ^3-carene SOA can be divided into four groups (Fig. S4), comparable to that of limonene SOA. Most of the SOA molecules are monomers ($\sim 70\%$) and dimers ($\sim 25\%$), while trimers and tetramers contribute to smaller proportions ($\sim 2\%$ and $< 1\%$, respectively) (Table S2). Although the SOA mass concentration increases by $\sim 100\%$ under high-RH conditions, the relative intensities of MS peaks do not significantly change with varying RH conditions. In other words, we did not observe an obvious change in the overall MS patterns, and the fractions of the four groups only slightly differed under different RH conditions; e.g., the fraction of monomers was 62 % under dry conditions and 66 % under wet conditions. However, if we take a closer look, the intensities and contributions of specific peaks are quite different with varying RH. For example, the relative intensity of $C_{10}H_{16}O_2$, a possible first-generation product (Gong et al., 2018), decreases by $\sim 20\%$ with increasing RH from dry to 60 % (Table S3). This is likely due to the multi-generation reactions influenced by water vapor concentration, as discussed below with the proposed reaction mechanism of limonene ozonolysis.

The proposed reaction mechanism of limonene ozonolysis is shown in Figs. 3 and 4. The initial step in the reaction of O_3 with limonene is the attack of the endocyclic double bond to form eCI_1 and eCI_2 (excited Criegee intermediates, with branching ratios of 0.35 and 0.65, respec-
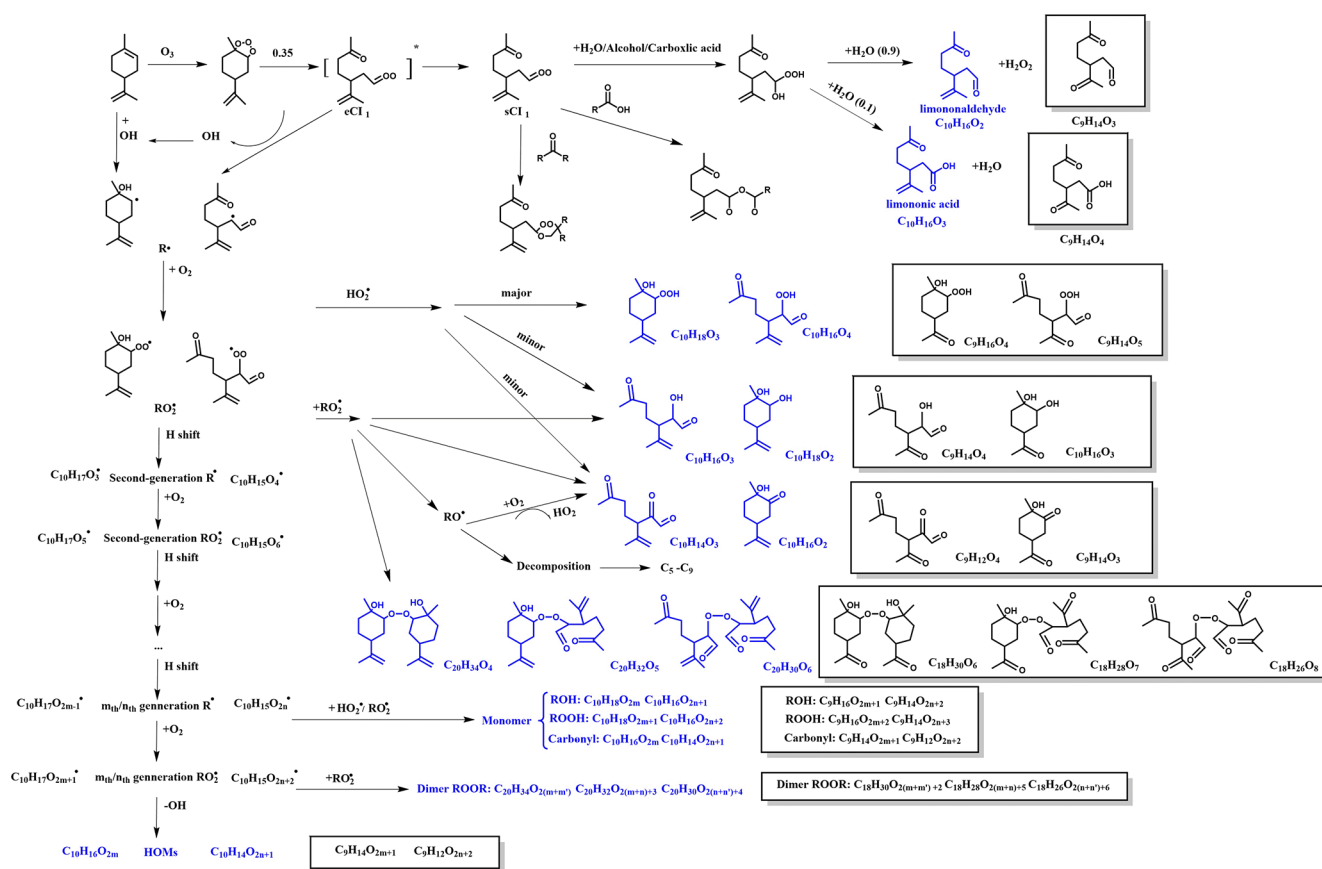
Figure 3. Proposed formation mechanism for SOA formation from eCI_1 oxidation under high RH. The compounds in blue and in boxes are identified using UPLC/($-$) ESI-Q-TOF-MS.

tively). In the context of eCI_1, several complex reactions occur, with the most dominant reaction being the generation of hydroxyl radicals (OH) and a reaction pathway known as sCI_1. The sCI_1 pathway can proceed through three distinct reactions, as depicted in Fig. 3. The first pathway is the reaction with H_2O, alcohol, or carboxylic acid to form a carboxylic acid species with hydroxyl, which would subsequently lose a molecule of water to form limononaldehyde or lose a molecule of hydrogen peroxide to form limononic acid (Grosjean et al., 1992; X. Li et al., 2019). The second and third pathways involve reactions of sCI_1 with carboxylic acids and carbonyls, respectively, leading to the formation of anhydrides and secondary ozonides. Additionally, the generated OH radicals can react with limonene, giving rise to another alkyl radical, $C_{10}H_{17}O\cdot$. These alkyl radicals react with O_2 and form peroxy radicals ($RO_2\cdot$). The atmospheric fate of produced $RO_2\cdot$ in the absence of NO_x includes the reaction with $RO_2\cdot$ or $HO_2\cdot$ (Atkinson and Arey, 2003) and the unimolecular H shift. The $RO_2\cdot + HO_2\cdot$ route mainly forms hydroperoxide (ROOH), and the minor fraction forms alcohols and carbonyls (Atkinson and Arey, 2003). The products of bimolecular reactions between $RO_2\cdot$ and $RO_2\cdot$ are alcohols, carbonyls, alkoxy radicals, peroxides, and ROOR

dimers (Hammes et al., 2019; Peng et al., 2019). The H shift of $RO_2\cdot$ can form second-generation $R\cdot$ and trigger a main generation channel of highly oxidized molecules (HOMs); i.e., $R\cdot$ would go through a process of repeated oxygen addition and hydrogen-atom shift to form HOMs with high O/C ratios of > 0.7–0.8 (Molteni et al., 2018; Bianchi et al., 2019).

In addition to the eCI_1 route, the eCI_2 pathway is also responsible for the generation of various products (Fig. 4). Since the reaction of the hydroxyl radical (OH) attacking limonene is already depicted in Fig. 3, our main emphasis in Fig. 4 is on the pathways involved in the generation of SCI. First, sCI_2 reacts with H_2O and decomposes to limononaldehyde and H_2O_2. Additionally, sCI_2 could experience an O_2 addition, $\cdot$OH loss, and isomerization to produce two types of $RO_2\cdot$, which can undergo the similar reactions as the $RO_2\cdot$ formed from the sCI_1 route, and the major products are also shown in Fig. 4.

Since limonene and Δ^3-carene both have an endocyclic double bond, similar reactions to those mentioned above can occur for the ozonolysis of Δ^3-carene (Fig. S5), and most corresponding formulas in Fig. S5 can be identified in Table S4. However, the reactivity of limonene towards O_3 is
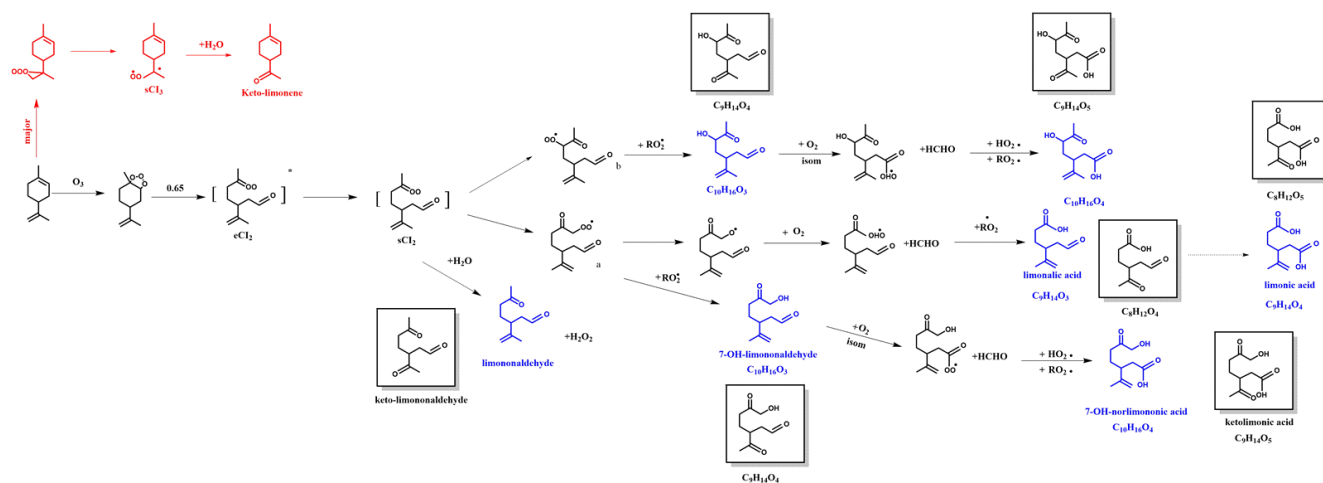
Figure 4. Proposed formation mechanisms for SOA formation from eCI$_2$ and exocyclic double-bond oxidation under high RH. The compounds in blue and in boxes are identified using UPLC/(−) ESI-Q-TOF-MS.

expected to be higher owing to its exocyclic double bond. As shown in Fig. 4, the attack of O$_3$ of the exocyclic double bond mainly leads to sCI$_3$ (highlighted in red), with the unpaired electrons outside the ring (Leungsakul et al., 2005). sCI$_3$ can react with H$_2$O to form a carbonyl called keto-limonene. It should be noted that this reaction can occur not only for limonene but also for all the products that retain the exocyclic double bond. As a result, the compounds that are colored in blue in Figs. 3 and 4 can undergo further reactions to generate products with an additional carbonyl (see the boxes in Figs. 3 and 4). Furthermore, their molecular formulas shown in Table S5 have been identified using the Q-TOF-MS. This mechanism can explain the decrease in the relative intensity of C$_{10}$H$_{16}$O$_2$ well from high RH to low RH and the increase in the relative intensity of C$_9$H$_{14}$O$_3$ from low RH to high RH (Table S3).

With such progress, we cannot rule out the possibility that relative humidity (RH) may influence the generation of other free radicals (Ma et al., 2009), thereby impacting the formation of secondary organic aerosols (SOAs), such as OH-radical reactions (Bonn et al., 2002; Fick et al., 2002). However, molar OH-radical yields were reported as 0.65 ± 0.10 (Hantschke et al., 2021), 0.86 ± 0.11 (Aschmann et al., 2002), and 0.56 to 0.59 (Wang et al., 2019) for Δ^3-carene, while for limonene, the reported yields were 0.67 ± 0.10 (Aschmann et al., 2002) and 0.76 ± 0.06 (Herrmann et al., 2010). It seems that the OH radicals produced from limonene and Δ^3-carene are quite similar within the range of uncertainties. Therefore, the increased ozone consumption by limonene seems primarily attributed to the presence of its exocyclic double bond.

3.3 Processes leading to the increase or decrease in SOA formation

Based on the results and mechanisms shown above, we present evidence that high humidity enhances limonene-SOA formation. First, the presence of water vapor enhances the formation of carbonyls from the reaction of exocyclic double bond, and the oligomerization of these carbonyls generates more dimers including hemiacetal (or acetal) formation and aldol condensation (Zhang et al., 2022; Kroll et al., 2005; Jang et al., 2003). As shown in Table S6, the intensity of dimers generating from multi-carbonyls under high RH is higher than that under low RH, and 54 out of the total 187 dimers were exclusively observed for limonene under high humidity conditions, contributing to a corresponding intensity of $\sim 19\%$ (Table S7). These dimers can be classified as low-volatility organic compounds (LVOCs; $3 \times 10^{-4} < C_0 < 0.3\,\mu\mathrm{g\,m^{-3}}$) and extremely low-volatile organic compounds (ELVOCs; $C_0 < 3 \times 10^{-4}\,\mu\mathrm{g\,m^{-3}}$) (Fig. 5a) and thus promote the nucleation and new particle formation in different ways. This finding is similar to that from a previous study showing that high RH can promote dimer formation from the ozonolysis of α-pinene (Kristensen et al., 2014). Second, we find that high RH can also promote the formation of HOMs, although the mechanism remains unclear. As shown in Table S3, many HOMs proposed from the mechanism are detected under high-RH conditions but not detected under low-RH conditions, including both monomers and dimers. Many HOMs have low volatilities and, thus, can also promote new particle formation. Overall, the promoted dimer and HOM formation may greatly enhance the new particle number concentration under high-RH conditions (Fig. 6).

High particle number concentration generally provides more surface areas for semi-volatile organic compounds
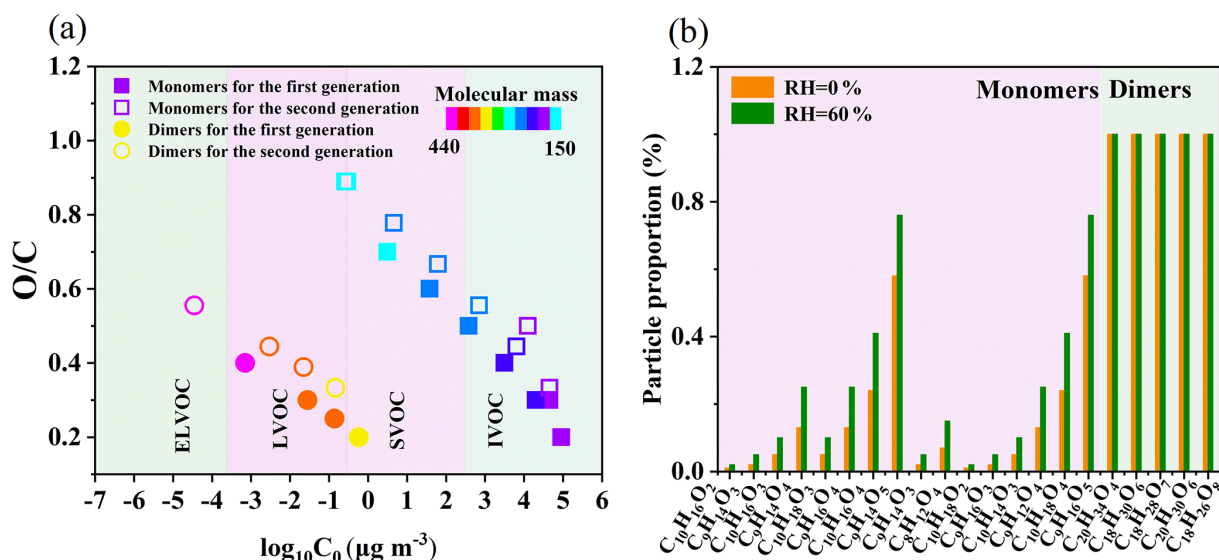
Figure 5. (a) Distribution of the limonene SOA in the two-dimensional volatility basis set (2D-VBS) space. (b) Partitioning coefficients of limonene monomers and dimers under low- and high-RH conditions.
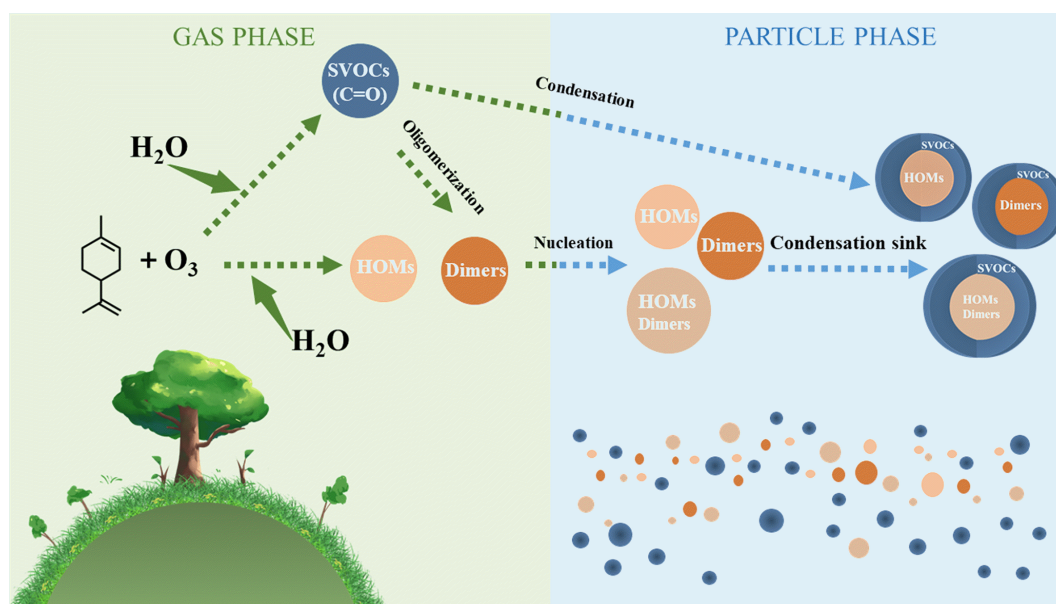

Figure 6. Schematic diagram of the possible mechanisms for the enhancement of limonene SOA.

(SVOCs; $0.3 < C_0 < 300\,\mu g\,m^{-3}$) to condense on, which results in a higher condensation sink (CS). In the OFR, the fates of SVOCs include condensing on aerosol, getting lost on the wall, and reacting with OH radicals to form functionalization and/or fragmentation products (Palm et al., 2016; K. Li et al., 2019). The promoted condensation by higher CS leads to a higher fraction of SVOCs getting into the particle phase rather than getting lost on the wall or becoming smaller fragments staying in the gas phase, thus promoting SOA formation (K. Li et al., 2019). Furthermore, the transformation from a C–C double bond to carbonyl shown in Figs. 3 and 4

decreases the volatility of molecules, which can largely influence the gas–particle partitioning of the monomeric compounds (Fig. 5b). For example, the C_0 values of $C_{10}H_{16}O_2$ and $C_{10}H_{16}O_3$ are 90 701 and 19 968 $\mu g\,m^{-3}$, corresponding to partitioning coefficients of 0.01 and 0.05, respectively (Fig. 5b and Table S3), with an SOA mass concentration of $\sim 1000\,\mu g\,m^{-3}$ under dry conditions. When they are converted to carbonyls $C_9H_{14}O_3$ and $C_9H_{14}O_4$, the values of C_0 become 45 556 and 6479 $\mu g\,m^{-3}$, corresponding to partitioning coefficients of 0.02 and 0.13, respectively (Fig. 5b and Table S3), with the same SOA loading. This enhance-

ment in partitioning coefficient can largely promote the condensation of SVOCs and, thus, enhance the SOA mass concentration. In addition, the enhanced SOA formation can further influence the equilibrium; e.g., the partitioning coefficient of $C_{10}H_{16}O_3$ increases from 0.05 to 0.10 when SOA mass concentration increases from $\sim 1000\,\mu g\,m^{-3}$ under dry conditions to $\sim 2000\,\mu g\,m^{-3}$ under wet conditions (Fig. 5b and Table S3). The distribution of saturation vapor pressure for monomers and dimers identified by MS has also been shown in Fig. 5a. As can be seen from this figure, around 50 % monomers are categorized as SVOCs, thus having the large fraction in the particle phase when converting from dry to wet conditions. Overall, it is likely that the different fate and partitioning of SVOCs largely enhance the amount of SVOCs in the particle phase (Fig. 6).

Concluding the analysis above, high humidity promotes the SOA formation from the ozonolysis of limonene in two steps: nucleation of new particles and condensation of SVOCs on them (Fig. 6). While our study highlights significant changes in gas-phase chemistry, we cannot exclude the possibility of concurrent reactions occurring in the condensed phase. These two steps are closely related to the multi-generation reactions of the exocyclic $C = C$ bond, which are unlikely to happen for the ozonolysis of Δ^3-carene. Interestingly, Gong and Chen (2021) have found that high RH can inhibit the SOA formation from the first-generation oxidation of limonene ozonolysis but enhance the SOA formation from the second-generation oxidation (Gong and Chen, 2021); their results agree well with the results and analysis shown here. In contrast, X. Li et al. (2019) found negligible change in dimers and HOMs in limonene-O_3 system when changing RH from 0 % to 60 %. The discrepancy is mainly attributed to the different experimental conditions. The ozone exposure in this study is ~ 18 times higher than in X. Li et al. (2019), while the limonene concentration in this study is only ~ 30 % of that in their study. These two conditions both favor the multi-generation reactions that occurred at the exocyclic double bond of limonene and its products. Thus, we believe this leads to the different results regarding the formation of HOMs and dimers.

Regarding Δ^3-carene, the mechanisms and processes are almost opposite to those of limonene. First, water vapor reacts with sCI_1 or sCI_2 to promote the formation of α-hydroxyalkyl–hydroperoxides (Fig. S5). Their subsequent products without second ozonolysis of exocyclic double bond have higher volatility and may most likely prevail in the gas phase. In addition, it has been found that α-hydroxyalkyl–hydroperoxides preferentially decompose into aldehydes and H_2O_2 (Kumar et al., 2014; Chen et al., 2016), i.e., 3-caronaldehyde for Δ^3-carene, which has higher volatility than the products from other reaction pathways. Correspondingly, the number and relative intensity of HOMs and dimers detected under high-RH conditions are both lower than those under low-RH conditions (Table S8). Furthermore, out of a total of 178 dimers, 63 dimers were ex-

clusively identified under low-RH conditions (Table S7). As a result, high RH shows an inhibitory effect on the SOA formation from Δ^3-carene ozonolysis.

To investigate the multi-generation reactions of limonene under low-concentration conditions, we conducted low-concentration limonene ozonolysis experiments, and the results are shown in Fig. S6. In these experiments, the limonene and O_3 concentrations were 20.5 ppb and 5.7 ppm, respectively. According to the experimental results, the number concentration of SOA formed from limonene ozonolysis increased by approximately 1.4 times under high RH, which is similar to the increase observed under high-loading conditions. The mass concentration increased by approximately 1.3 times at a precursor concentration of 20.5 ppb. The relatively small increase in mass concentration compared to the high-concentration conditions may be attributed to the less pronounced distribution of SVOCs at low mass concentrations. This result suggests that the enhancement effect on limonene SOA by high RH is still valid for low precursor concentrations.

To further confirm the assumption that water-influenced multi-generation reactions of the exocyclic double bond enhance the SOA formation, we conducted two comparative analyses: firstly, we examined the ozonolysis of the endocyclic double bond in limonene, leaving the exocyclic double bond unreacted. This was done by applying a low O_3 concentration (~ 67 ppb), since the reaction of O_3 with an endocyclic double bond is ~ 30 times faster than the reaction of O_3 with an exocyclic double bond (Shu and Atkinson, 1994). Interestingly, when limonene was oxidized at only the endocyclic double bond, we observed a slight decrease in both the number and mass concentrations as the RH increased (Fig. S7). This is similar to the results obtained for Δ^3-carene, which contains only one endocyclic double bond. Secondly, we compared the ozonolysis of structurally similar β-caryophyllene, which has an exocyclic C–C double bond that can undergo further reactions (Fig. S8). As expected, we observe a large enhancement in SOA formation under high-RH conditions (Table S9 and Fig. S9). This implies that monoterpenes, sesquiterpenes, and other BVOCs with two unsaturation double bonds may follow similar reaction mechanisms during ozonolysis and thus have a RH dependency in SOA production.

4 Conclusions

In this study, the effect of humidity on SOA production from the ozonolysis of two monoterpenes (limonene and Δ^3-carene) was investigated with an OFR. Contrasting impacts of RH on the SOA formation were observed: limonene-SOA yield increases by ~ 100 % when RH changes from ~ 1 % to ~ 60 %, while Δ^3-carene-SOA yield slightly decreases. By analyzing the chemical composition of SOA with ESI-Q-TOF-MS, we find that the multi-generation reactions of

the exocyclic C–C double bond are likely the driving force of the enhancement in limonene SOA. The presence of water promotes the formation of carbonyls from the reaction of exocyclic double bond and further favors the formation of dimers and HOMs. This leads to promoted new particle formation and subsequent condensation of SVOCs. These reactions also lower the volatilities of the SVOCs and further promote the gas–particle partitioning. Moreover, this hypothesis is supported by a similar behavior of the ozonolysis of β-caryophyllene (sesquiterpene with an exocyclic double bond) in SOA enhancement under high-RH conditions. However, since aerosol dynamics of small clusters and particles are very complex, we do not rule out a series of reactions that may occur in the particle phase. The results in this study suggest that multi-generation reactions play an important role in SOA formation from the ozonolysis of BVOCs, which are significantly influenced by humidity. This impact is largely dependent on the molecular structure of the SOA precursors (e.g., with or without the exocyclic double bond), thus highlighting the importance of considering the molecular structure of monoterpenes in modeling and field studies of biogenic SOA.

Author contributions. LD and SZ designed the experiments, and SZ carried them out. SZ performed data analysis with assistance from KL, LD, ZY, and JL. SZ and KL wrote the paper with contributions from all co-authors.

References

Ahmadov, R., McKeen, S. A., Robinson, A. L., Bahreini, R., Middlebrook, A. M., de Gouw, J. A., Meagher, J., Hsie, E. Y., Edgerton, E., Shaw, S., and Trainer, M.: A volatility basis set model for summertime secondary organic aerosols over the eastern United States in 2006, J. Geophys. Res.-Atmos., 117, D6301, https://doi.org/10.1029/2011JD016831, 2012.

Aschmann, S. M., Arey, J., and Atkinson, R.: OH radical formation from the gas-phase reactions of O_3 with a series of terpenes, Atmos. Environ., 36, 4347–4355, https://doi.org/10.1016/S1352-2310(02)00355-2, 2002.

Atkinson, R.: Kinetics and mechanisms of the gas-phase reactions of the NO_3 radical with organic compounds, J. Phys. Chem. Ref. Data, 20, 459–507, https://doi.org/10.1063/1.555887, 1991.

Atkinson, R. and Arey, J.: Gas-phase tropospheric chemistry of biogenic volatile organic compounds: a review, Atmos. Environ., 37, 197–219, https://doi.org/10.1016/S1352-2310(03)00391-1, 2003.

Bäck, J., Aalto, J., Henriksson, M., Hakola, H., He, Q., and Boy, M.: Chemodiversity of a Scots pine stand and implications for terpene air concentrations, Biogeosciences, 9, 689–702, https://doi.org/10.5194/bg-9-689-2012, 2012.

Bateman, A. P., Nizkorodov, S. A., Laskin, J., and Laskin, A.: Time-resolved molecular characterization of limonene/ozone aerosol using high-resolution electrospray ionization mass spectrometry, Phys. Chem. Chem. Phys., 11, 7931–7942, https://doi.org/10.1039/b905288g, 2009.

Bianchi, F., Kurtén, T., Riva, M., Mohr, C., Rissanen, M. P., Roldin, P., Berndt, T., Crounse, J. D., Wennberg, P. O., Mentel, T. F., Wildt, J., Junninen, H., Jokinen, T., Kulmala, M., Worsnop, D. R., Thornton, J. A., Donahue, N., Kjaergaard, H. G., and Ehn, M.: Highly oxygenated organic molecules (HOM) from gas-phase autoxidation involving peroxy radicals: a key contributor to atmospheric aerosol, Chem. Rev., 119, 3472–3509, https://doi.org/10.1021/acs.chemrev.8b00395, 2019.

Bonn, B. and Moortgat, G. K.: New particle formation during α- and β-pinene oxidation by O_3, OH and NO_3, and the influence of water vapour: particle size distribution studies, Atmos. Chem. Phys., 2, 183–196, https://doi.org/10.5194/acp-2-183-2002, 2002.

Bonn, B., Schuster, G., and Moortgat, G. K.: Influence of water vapor on the process of new particle formation during monoterpene ozonolysis, J. Phys. Chem. A, 106, 2869–2881, https://doi.org/10.1021/jp012713p, 2002.

Chen, H., Ren, Y., Cazaunau, M., Dalele, V., Hu, Y., Chen, J., and Mellouki, A.: Rate coefficients for the reaction of ozone with 2-and 3-carene, Chem. Phys. Lett., 621, 71–77, https://doi.org/10.1016/j.cplett.2014.12.056, 2015.

Chen, L., Huang, Y., Xue, Y., Shen, Z., Cao, J., and Wang, W.: Mechanistic and kinetics investigations of oligomer for-

mation from Criegee intermediate reactions with hydroxyalkyl hydroperoxides, Atmos. Chem. Phys., 19, 4075–4091, https://doi.org/10.5194/acp-19-4075-2019, 2019.

Chen, L., Wang, W., Wang, W., Liu, Y., Liu, F., Liu, N., and Wang, B.: Water-catalyzed decomposition of the simplest Criegee intermediate CH_2OO, Theor. Chem. Acc., 135, 131, https://doi.org/10.1007/s00214-016-1894-9, 2016.

Chen, X. and Hopke, P. K.: A chamber study of secondary organic aerosol formation by limonene ozonolysis, Indoor Air, 20, 320–328, https://doi.org/10.1111/j.1600-0668.2010.00656.x, 2010.

Cholakian, A., Beekmann, M., Coll, I., Ciarelli, G., and Colette, A.: Biogenic secondary organic aerosol sensitivity to organic aerosol simulation schemes in climate projections, Atmos. Chem. Phys., 19, 13209–13226, https://doi.org/10.5194/acp-19-13209-2019, 2019.

de Matos, S. P., Teixeira, H. F., de Lima, Á. A. N., Veiga-Junior, V. F., and Koester, L. S.: Essential oils and isolated terpenes in nanosystems designed for topical administration: a review, Biomolecules, 9, 138, https://doi.org/10.3390/biom9040138, 2019.

Drozd, G. T. and Donahue, N. M.: Pressure dependence of stabilized Criegee intermediate formation from a sequence of alkenes, J. Phys. Chem. A, 115, 4381–4387, https://doi.org/10.1021/jp2001089, 2011.

Fick, J., Pommer, L., Andersson, B., and Nilsson, C.: A study of the gas-phase ozonolysis of terpenes: the impact of radicals formed during the reaction, Atmos. Environ., 36, 3299–3308, https://doi.org/10.1016/s1352-2310(02)00291-1, 2002.

Gong, Y. and Chen, Z.: Quantification of the role of stabilized Criegee intermediates in the formation of aerosols in limonene ozonolysis, Atmos. Chem. Phys., 21, 813–829, https://doi.org/10.5194/acp-21-813-2021, 2021.

Gong, Y., Chen, Z., and Li, H.: The oxidation regime and SOA composition in limonene ozonolysis: roles of different double bonds, radicals, and water, Atmos. Chem. Phys., 18, 15105–15123, https://doi.org/10.5194/acp-18-15105-2018, 2018.

Grosjean, D., Williams, E. L., and Seinfeld, J. H.: Atmospheric oxidation of selected terpenes and related carbonyls: gas-phase carbonyl products, Environ. Sci. Technol., 26, 1526–1533, https://doi.org/10.1021/es00032a005, 1992.

Guenther, A. B., Jiang, X., Heald, C. L., Sakulyanontvittaya, T., Duhl, T., Emmons, L. K., and Wang, X.: The model of emissions of gases and aerosols from nature version 2.1 (MEGAN2.1): an extended and updated framework for modeling biogenic emissions, Geosci. Model Dev., 5, 1471–1492, https://doi.org/10.5194/gmd-5-1471-2012, 2012.

Guo, S., Hu, M., Zamora, M. L., Peng, J., Shang, D., Zheng, J., Du, Z., Wu, Z., Shao, M., Zeng, L., Molina, M. J., and Zhang, R.: Elucidating severe urban haze formation in China, P. Natl. Acad. Sci. USA, 111, 17373–17378, https://doi.org/10.1073/pnas.1419604111, 2014.

Hammes, J., Lutz, A., Mentel, T., Faxon, C., and Hallquist, M.: Carboxylic acids from limonene oxidation by ozone and hydroxyl radicals: insights into mechanisms derived using a FIGAERO-CIMS, Atmos. Chem. Phys., 19, 13037–13052, https://doi.org/10.5194/acp-19-13037-2019, 2019.

Hantschke, L., Novelli, A., Bohn, B., Cho, C., Reimer, D., Rohrer, F., Tillmann, R., Glowania, M., Hofzumahaus, A., Kiendler-Scharr, A., Wahner, A., and Fuchs, H.: Atmospheric photooxi-

dation and ozonolysis of Δ3-carene and 3-caronaldehyde: rate constants and product yields, Atmos. Chem. Phys., 21, 12665–12685, https://doi.org/10.5194/acp-21-12665-2021, 2021.

Herrmann, F., Winterhalter, R., Moortgat, G. K., and Williams, J.: Hydroxyl radical (OH) yields from the ozonolysis of both double bonds for five monoterpenes, Atmos. Environ., 44, 3458–3464, https://doi.org/10.1016/j.atmosenv.2010.05.011, 2010.

Huang, X., Yun, H., Gong, Z., Li, X., He, L., Zhang, Y., and Hu, M.: Source apportionment and secondary organic aerosol estimation of $PM_{2.5}$ in an urban atmosphere in China, Sci. China-Earth Sci., 57, 1352–1362, https://doi.org/10.1007/s11430-013-4686-2, 2014.

Jang, M. S., Carroll, B., Chandramouli, B., and Kamens, R. M.: Particle growth by acid-catalyzed heterogeneous reactions of organic carbonyls on preexisting aerosols, Environ. Sci. Technol., 37, 3828–3837, https://doi.org/10.1021/es021005u, 2003.

Jokinen, T., Berndt, T., Makkonen, R., Kerminen, V.-M., Junninen, H., Paasonen, P., Stratmann, F., Herrmann, H., Guenther, A. B., Worsnop, D. R., Kulmala, M., Ehn, M., and Sipilä, M.: Production of extremely low volatile organic compounds from biogenic emissions: Measured yields and atmospheric implications, P. Natl. Acad. Sci. USA, 112, 7123–7128, https://doi.org/10.1073/pnas.1423977112, 2015.

Jonsson, A. M., Hallquist, M., and Ljungstrom, E.: Impact of humidity on the ozone initiated oxidation of limonene, Δ^3-carene, and α-pinene, Environ. Sci. Technol., 40, 188–194, https://doi.org/10.1021/es051163w, 2006.

Jonsson, A. M., Hallquist, M., and Ljungstrom, E.: Influence of OH scavenger on the water effect on secondary organic aerosol formation from ozonolysis of limonene, Δ^3-carene, and α-pinene, Environ. Sci. Technol., 42, 5938–5944, https://doi.org/10.1021/es702508y, 2008.

Kanakidou, M., Seinfeld, J. H., Pandis, S. N., Barnes, I., Dentener, F. J., Facchini, M. C., Van Dingenen, R., Ervens, B., Nenes, A., Nielsen, C. J., Swietlicki, E., Putaud, J. P., Balkanski, Y., Fuzzi, S., Horth, J., Moortgat, G. K., Winterhalter, R., Myhre, C. E. L., Tsigaridis, K., Vignati, E., Stephanou, E. G., and Wilson, J.: Organic aerosol and global climate modelling: a review, Atmos. Chem. Phys., 5, 1053–1123, https://doi.org/10.5194/acp-5-1053-2005, 2005.

Khamaganov, V. G. and Hites, R. A.: Rate constants for the gas-phase reactions of ozone with isoprene, α- and β-pinene, and limonene as a function of temperature, J. Phys. Chem. A, 105, 815–822, https://doi.org/10.1021/jp002730z, 2001.

Kristensen, K., Cui, T., Zhang, H., Gold, A., Glasius, M., and Surratt, J. D.: Dimers in α-pinene secondary organic aerosol: effect of hydroxyl radical, ozone, relative humidity and aerosol acidity, Atmos. Chem. Phys., 14, 4201–4218, https://doi.org/10.5194/acp-14-4201-2014, 2014.

Kroll, J. H., Ng, N. L., Murphy, S. M., Varutbangkul, V., Flagan, R. C., and Seinfeld, J. H.: Chamber studies of secondary organic aerosol growth by reactive uptake of simple carbonyl compounds, J. Geophys. Res.-Atmos., 110, D23207, https://doi.org/10.1029/2005JD006004, 2005.

Kumar, M., Busch, D. H., Subramaniam, B., and Thompson, W. H.: Role of tunable acid catalysis in decomposition of α-Hydroxyalkyl hydroperoxides and mechanistic implications for tropospheric chemistry, J. Phys. Chem. A, 118, 9701–9711, https://doi.org/10.1021/jp505100x, 2014.

Leungsakul, S., Jaoui, M., and Kamens, R. M.: Kinetic Mechanism for Predicting Secondary Organic Aerosol Formation from the Reaction of d-Limonene with Ozone, Environ. Sci. Technol., 39, 9583–9594, https://doi.org/10.1021/es0492687, 2005.

Levy II, H., Horowitz, L. W., Schwarzkopf, M. D., Ming, Y., Golaz, J.-C., Naik, V., and Ramaswamy, V.: The roles of aerosol direct and indirect effects in past and future climate change, J. Geophys. Res.-Atmos., 118, 4521–4532, https://doi.org/10.1002/jgrd.50192, 2013.

Li, J. Y., Zhang, H. W., Ying, Q., Wu, Z. J., Zhang, Y. L., Wang, X. M., Li, X. H., Sun, Y. L., Hu, M., Zhang, Y. H., and Hu, J. L.: Impacts of water partitioning and polarity of organic compounds on secondary organic aerosol over eastern China, Atmos. Chem. Phys., 20, 7291–7306, https://doi.org/10.5194/acp-20-7291-2020, 2020.

Li, K., Liggio, J., Lee, P., Han, C., Liu, Q., and Li, S.-M.: Secondary organic aerosol formation from α-pinene, alkanes, and oil-sands-related precursors in a new oxidation flow reactor, Atmos. Chem. Phys., 19, 9715–9731, https://doi.org/10.5194/acp-19-9715-2019, 2019.

Li, X., Chee, S., Hao, J., Abbatt, J. P. D., Jiang, J., and Smith, J. N.: Relative humidity effect on the formation of highly oxidized molecules and new particles during monoterpene oxidation, Atmos. Chem. Phys., 19, 1555–1570, https://doi.org/10.5194/acp-19-1555-2019, 2019.

Liu, Q., Liggio, J., Breznan, D., Thomson, E. M., Kumarathasan, P., Vincent, R., Li, K., and Li, S.-M.: Oxidative and Toxicological Evolution of Engineered Nanoparticles with Atmospherically Relevant Coatings, Environ. Sci. Technol., 53, 3058–3066, https://doi.org/10.1021/acs.est.8b06879, 2019.

Liu, Y., Liggio, J., Harner, T., Jantunen, L., Shoeib, M., and Li, S.-M.: Heterogeneous OH Initiated Oxidation: A Possible Explanation for the Persistence of Organophosphate Flame Retardants in Air, Environ. Sci. Technol., 48, 1041–1048, https://doi.org/10.1021/es404515k, 2014.

Ma, Y., Porter, R. A., Chappell, D., Russell, A. T., and Marston, G.: Mechanisms for the formation of organic acids in the gas-phase ozonolysis of 3-carene, Phys. Chem. Chem. Phys., 11, 4184–4197, https://doi.org/10.1039/b818750a, 2009.

Molteni, U., Bianchi, F., Klein, F., El Haddad, I., Frege, C., Rossi, M. J., Dommen, J., and Baltensperger, U.: Formation of highly oxygenated organic molecules from aromatic compounds, Atmos. Chem. Phys., 18, 1909–1921, https://doi.org/10.5194/acp-18-1909-2018, 2018.

Mot, M.-D., Gavrilaş, S., Lupitu, A. I., Moisa, C., Chambre, D., Tit, D. M., Bogdan, M. A., Bodescu, A.-M., Copolovici, L., Copolovici, D. M., and Bungau, S. G.: Salvia officinalis L. essential oil: characterization, antioxidant properties, and the effects of aromatherapy in adult patients, Antioxidants, 11, 808, https://doi.org/10.3390/antiox11050808, 2022.

Ng, N. L., Kroll, J. H., Chan, A. W. H., Chhabra, P. S., Flagan, R. C., and Seinfeld, J. H.: Secondary organic aerosol formation from m-xylene, toluene, and benzene, Atmos. Chem. Phys., 7, 3909–3922, https://doi.org/10.5194/acp-7-3909-2007, 2007.

Odum, J. R., Hoffmann, T., Bowman, F., Collins, D., Flagan, R. C., and Seinfeld, J. H.: Gas/particle partitioning and secondary organic aerosol yields, Environ. Sci. Technol., 30, 2580–2585, https://doi.org/10.1021/es950943+, 1996.

Palm, B. B., Campuzano-Jost, P., Ortega, A. M., Day, D. A., Kaser, L., Jud, W., Karl, T., Hansel, A., Hunter, J. F., Cross, E. S., Kroll, J. H., Peng, Z., Brune, W. H., and Jimenez, J. L.: In situ secondary organic aerosol formation from ambient pine forest air using an oxidation flow reactor, Atmos. Chem. Phys., 16, 2943–2970, https://doi.org/10.5194/acp-16-2943-2016, 2016.

Pathak, R. K., Salo, K., Emanuelsson, E. U., Cai, C., Lutz, A., Hallquist, A. M., and Hallquist, M.: Influence of ozone and radical chemistry on limonene organic aerosol production and thermal characteristics, Environ. Sci. Technol., 46, 11660–11669, https://doi.org/10.1021/es301750r, 2012.

Peng, Z., Lee-Taylor, J., Orlando, J. J., Tyndall, G. S., and Jimenez, J. L.: Organic peroxy radical chemistry in oxidation flow reactors and environmental chambers and their atmospheric relevance, Atmos. Chem. Phys., 19, 813–834, https://doi.org/10.5194/acp-19-813-2019, 2019.

Pye, H. O. T., Ward-Caviness, C. K., Murphy, B. N., Appel, K. W., and Seltzer, K. M.: Secondary organic aerosol association with cardiorespiratory disease mortality in the United States, Nat. Commun., 12, 7215, https://doi.org/10.1038/s41467-021-27484-1, 2021.

Ravichandran, C., Badgujar, P. C., Gundev, P., and Upadhyay, A.: Review of toxicological assessment of d-limonene, a food and cosmetics additive, Food Chem. Toxicol., 120, 668–680, https://doi.org/10.1016/j.fct.2018.07.052, 2018.

Sbai, S. E. and Farida, B.: Photochemical aging and secondary organic aerosols generated from limonene in an oxidation flow reactor, Environ. Sci. Pollut. Res., 26, 18411-18420, https://doi.org/10.1007/s11356-019-05012-5, 2019.

Seinfeld, J. H., Erdakos, G. B., Asher, W. E., and Pankow, J. F.: Modeling the formation of secondary organic aerosol (SOA). 2. The predicted effects of relative humidity on aerosol formation in the α-Pinene-, β-Pinene-, sabinene-, Δ^3-Carene-, and cyclohexene-ozone systems, Environ. Sci. Technol., 35, 1806–1817, https://doi.org/10.1021/es001765+, 2001.

Shaw, J. T., Lidster, R. T., Cryer, D. R., Ramirez, N., Whiting, F. C., Boustead, G. A., Whalley, L. K., Ingham, T., Rickard, A. R., Dunmore, R. E., Heard, D. E., Lewis, A. C., Carpenter, L. J., Hamilton, J. F., and Dillon, T. J.: A self-consistent, multivariate method for the determination of gas-phase rate coefficients, applied to reactions of atmospheric VOCs and the hydroxyl radical, Atmos. Chem. Phys., 18, 4039–4054, https://doi.org/10.5194/acp-18-4039-2018, 2018.

Shu, Y. G. and Atkinson, R.: Rate Constants for the gas-pahse reactions of O_3 with a series of terpenes and OH radical formation from the O_3 reactions with sesquiterpenes at 296 ± 2 K, Int. J. Chem. Kinet., 26, 1193–1205, https://doi.org/10.1002/kin.550261207, 1994.

Sindelarova, K., Granier, C., Bouarar, I., Guenther, A., Tilmes, S., Stavrakou, T., Müller, J. F., Kuhn, U., Stefani, P., and Knorr, W.: Global data set of biogenic VOC emissions calculated by the MEGAN model over the last 30 years, Atmos. Chem. Phys., 14, 9317–9341, https://doi.org/10.5194/acp-14-9317-2014, 2014.

Sun, Y., Wang, Z., Fu, P., Jiang, Q., Yang, T., Li, J., and Ge, X.: The impact of relative humidity on aerosol composition and evolution processes during wintertime in Beijing, China, Atmos. Environ., 77, 927–934, https://doi.org/10.1016/j.atmosenv.2013.06.019, 2013.

Thomsen, D., Elm, J., Rosati, B., Skonager, J. T., Bilde, M., and Glasius, M.: Large discrepancy in the formation of secondary organic aerosols from structurally similar monoterpenes, ACS Earth Space Chem., 5, 632–644, https://doi.org/10.1021/acsearthspacechem.0c00332, 2021.

Varutbangkul, V., Brechtel, F. J., Bahreini, R., Ng, N. L., Keywood, M. D., Kroll, J. H., Flagan, R. C., Seinfeld, J. H., Lee, A., and Goldstein, A. H.: Hygroscopicity of secondary organic aerosols formed by oxidation of cycloalkenes, monoterpenes, sesquiterpenes, and related compounds, Atmos. Chem. Phys., 6, 2367–2388, https://doi.org/10.5194/acp-6-2367-2006, 2006.

Wang, L., Liu, Y., and Wang, L.: Ozonolysis of 3-carene in the atmosphere. Formation mechanism of hydroxyl radical and secondary ozonides, Phys. Chem. Chem. Phys., 21, 8081–8091, https://doi.org/10.1039/c8cp07195k, 2019.

Wang, L. Y. and Wang, L. M.: The oxidation mechanism of gas-phase ozonolysis of limonene in the atmosphere, Phys. Chem. Chem. Phys., 23, 9294–9303, https://doi.org/10.1039/d0cp05803c, 2021.

Watne, A. K., Westerlund, J., Hallquist, A. M., Brune, W. H., and Hallquist, M.: Ozone and OH-induced oxidation of monoterpenes: Changes in the thermal properties of secondary organic aerosol (SOA), J. Aerosol Sci., 114, 31–41, https://doi.org/10.1016/j.jaerosci.2017.08.011, 2017.

Xu, L., Tsona, N. T., and Du, L.: Relative humidity changes the role of SO_2 in biogenic secondary organic aerosol formation, J. Phys. Chem. Lett., 12, 7365–7372, https://doi.org/10.1021/acs.jpclett.1c01550, 2021.

Ye, J., Abbatt, J. P. D., and Chan, A. W. H.: Novel pathway of SO_2 oxidation in the atmosphere: reactions with monoterpene ozonolysis intermediates and secondary organic aerosol, Atmos. Chem. Phys., 18, 5549–5565, https://doi.org/10.5194/acp-18-5549-2018, 2018.

Yu, K. P., Lin, C. C., Yang, S. C., and Zhao, P.: Enhancement effect of relative humidity on the formation and regional respiratory deposition of secondary organic aerosol, J. Hazard. Mater., 191, 94–102, https://doi.org/10.1016/j.jhazmat.2011.04.042, 2011.

Zhang, H., Wang, S., Hao, J., Wang, X., Wang, S., Chai, F., and Li, M.: Air pollution and control action in Beijing, J. Clean Prod., 112, 1519–1527, https://doi.org/10.1016/j.jclepro.2015.04.092, 2016.

Zhang, Y., He, L., Sun, X., Ventura, O. N., and Herrmann, H.: Theoretical Investigation on the Oligomerization of Methylglyoxal and Glyoxal in Aqueous Atmospheric Aerosol Particles, ACS Earth Space Chem., 6, 1031–1043, https://doi.org/10.1021/acsearthspacechem.1c00422, 2022.

Zhao, R. R., Zhang, Q. X., Xu, X. Z., Zhao, W. X., Yu, H., Wang, W. J., Zhang, Y. M., and Zhang, W. J.: Effect of experimental conditions on secondary organic aerosol formation in an oxidation flow reactor, Atmos. Pollut. Res., 12, 392–400, https://doi.org/10.1016/j.apr.2021.01.011, 2021.

Ziemann, P. J. and Atkinson, R.: Kinetics, products, and mechanisms of secondary organic aerosol formation, Chem. Soc. Rev., 41, 6582–6605, https://doi.org/10.1039/c2cs35122f, 2012.